

Chapter 3: Experimental route

3.1. Materials

Polyether sulfone (PES) Veradel 3300 was a gift sample from M/s Solvay Speciality Polymers Ltd., Vadodara, India. MWCNTs (diameter 6-9 nm) were commercial sample from M/s Sigma Aldrich, the surfactant Brij 98 (Sigma Aldrich), ethylene diamine (>99%, Sigma Aldrich), sodium azide (>99%, Sigma Aldrich), 1-pentyne (>99%, Sigma Aldrich), Bovine Serum Albumin (>99%, Sigma Aldrich) were used as received. Hydrochloric acid, Nitric acid, Thionyl chloride, Iso-propanol, Chlorosulfonic acid, Di-methyl formamide, Di-chloro methane and N-methyl pyrrolidone was purchased from Spectrochem Pvt. Ltd. and used as received.

3.2. Purification and functionalization of MWCNT

3.2.1. Surface cleaning

The purification of commercially purchased nanotubes is an important step to remove the unwanted side products during the preparation of nanotubes. The modified method have been used for the removal of these impurities like carbon soot, metal ions etc. 2 gm of nanotubes with 500 ml of 1 % Brij 98 (a non-ionic surfactant) were sonicated in the solution for the duration of 2h. The resulting solution was allowed to stand for 6h and the supernatant liquid was decanted followed by centrifugation at 3000 rpm for 15 minutes duration. The nanotubes free from impurities were taken and precipitates were rejected as it may contain soot. The process was repeated for 3 times to get the uncontaminated carbon nanotubes. Nanotubes were washed with water and brine solution alternatively which helps to remove the surfactant associated with them. The associated heavy metals were removed by converting them to soluble metal chlorides by the treatment of resulting solution with 0.5N HCl solution. The acid treated nanotubes do not get attracted to magnetic needle which confirms the removal of traces of Ni/Co/Fe which were present in the

Chapter 3: Experimental route

raw nanotubes. Finally uncontaminated nanotubes were dried in the vacuum oven at 80 °C for 10 h. Yield obtained was ~ 40%.

3.2.2. Oxidation, amide and azide functionalization of MWCNTs

The details of the various functionality attached to the MWCNTs are given in Table 3.1. To enhance the interaction between MWCNT and polymer, the purified MWCNTs were attached with three functional group (Figure 3.1). The initial step chosen was oxidation, as the carboxylated groups are easy to convert in other functional group e.g. ester, amide etc. [220]. For oxidation, purified nanotubes were treated with 3:1 mixture of concentrated nitric acid and sulphuric acid (40 ml) for 24 h at 33 °C. To get the clean surface of oxidized nanotubes the treated MWCNTs was washed with Deionized (DI) water 5 times. The product was dried in oven under vacuum at 80 °C temperature for 8 h. Percentage yield obtained was 58.2.

Further, acylation reaction is carried out to introduce acyl group on multiwalled carbon nanotubes. 200 mg of oxidized nanotubes are treated with 20 ml of thionyl chloride and 2 ml of N, N-Dimethyl formamide (DMF) in a round bottom flask. The reaction was kept under stirring for 36 h at 60 °C temperature. The effluent was washed with toluene to remove the excess thionyl chloride. Nanotubes were collected by centrifugation at the speed of 3000 rotation per minute. The resulting product was dried in oven under vacuum at 80 °C for 8 h.

For amide functionalization 20 mg of Acylated MWCNT was dispersed in 10 ml ethylene diamine and sonication is done for 16 h at 33 °C, in a fuming hood. 200 ml methanol was added to the reaction mixture. Amide functionalized MWCNTs was obtained by centrifugation at 3000 rotation per minute speed. Product was dried in vacuum oven at 80°C for 8 h with 70.3% yield. To add azide functional group 60 mg of Acylated MWCNT and 5 mg of sodium azide was added to DMF in round bottom flask under stirring and

Chapter 3: Experimental route

reaction was performed at Room Temperature for 24 h. DMF was used as solvent. The product was dried in vacuum oven at 80 °C for 8 h. Yield was 77.5%. Functionalizations of MWCNTs were confirmed by FTIR analysis.

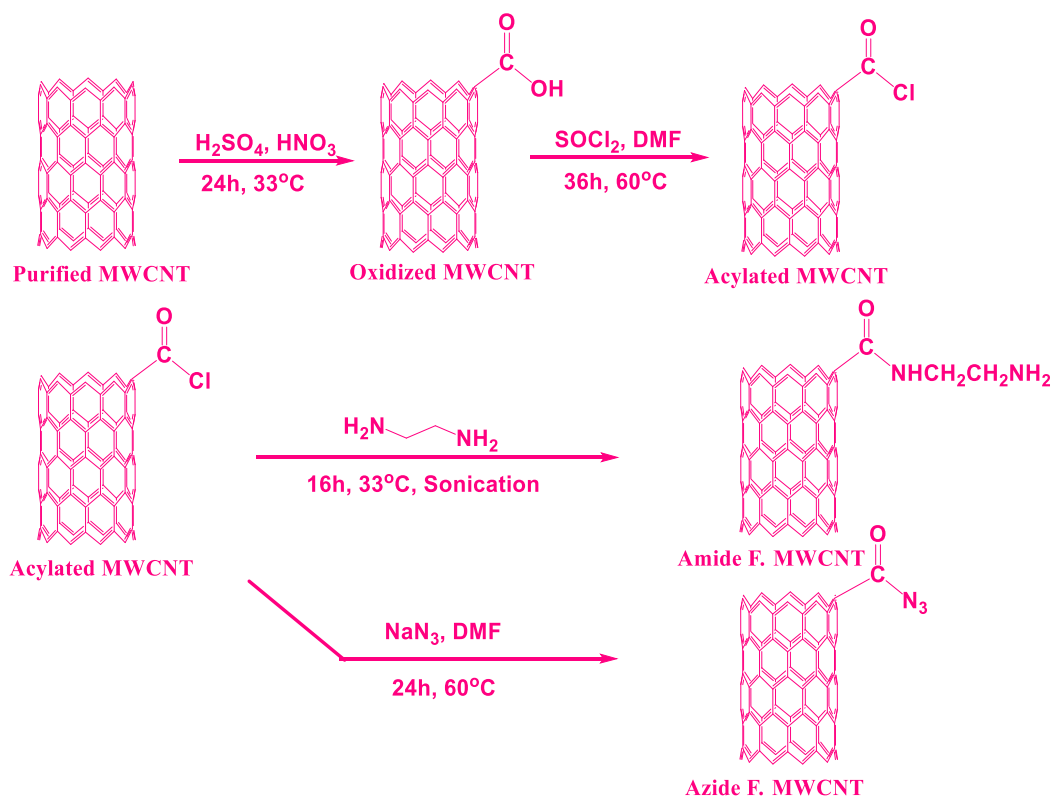


Figure 3.1 Schematic representation of different steps of functionalized MWCNT

3.2.3. Incorporation of f-MWCNT into polyethersulfone to form mixed matrix membranes

Poly ether sulfone was dried in vacuum oven at 80 °C for 24 h to remove moisture associated with the polymer. Dimethyl formamide was used as solvent to dissolve the polymer. 1% iso-propanol in de-ionized (DI) water was

Chapter 3: Experimental route

used as coagulation bath. 18wt% PES was dissolved in DMF under stirring at 50 °C in reaction vessel. A viscous dope solution was formed. Different weight percentage of all the functionalized MWCNT was added to the polymer dope solution. Mixed matrix membranes were prepared according to the classical dry/wet phase inversion process (Figure 3.2). The membrane dope solutions sonicated in an ultrasonic device for 12 h for well dispersion of nanotubes and to obtain homogeneous solution. The mixed matrix membranes were casted on a glass plate using casting knife to prepare flat sheet film of homogeneous thickness. The film was exposed to air for 10 minutes for the solvent evaporation followed by immersion in coagulation water bath containing 1% iso-propanol where the solvent non-solvent exchange takes place.

The membranes were washed with DI water and dried at 80°C temperature in vacuum oven and kept soaked in deionised water for further studies. The images of the prepared membranes are shown in Figure 3.3 and 3.4.

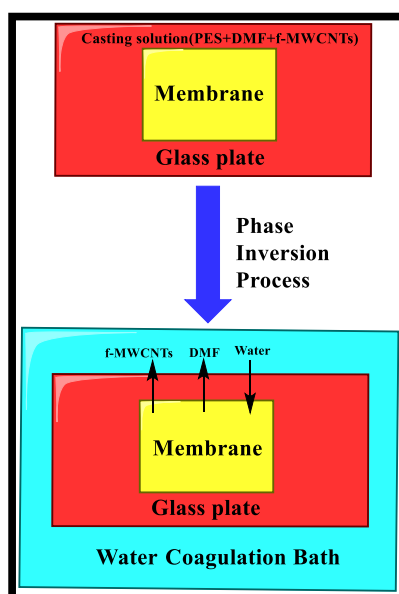


Figure 3.2 Illustration of phase inversion process for membrane preparation

Chapter 3: Experimental route

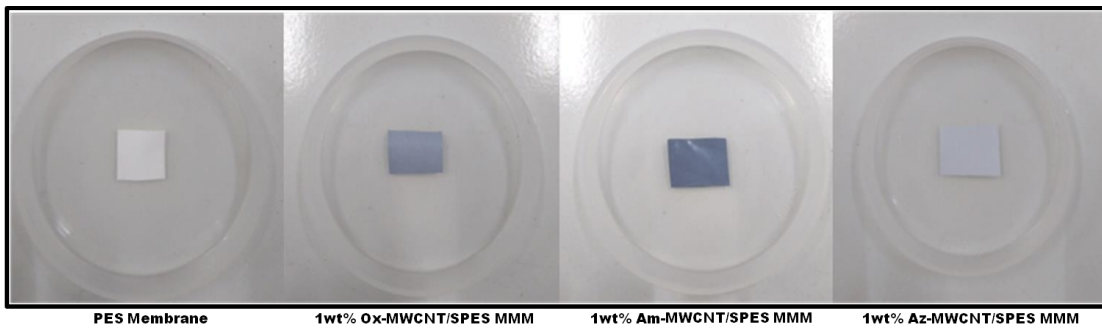
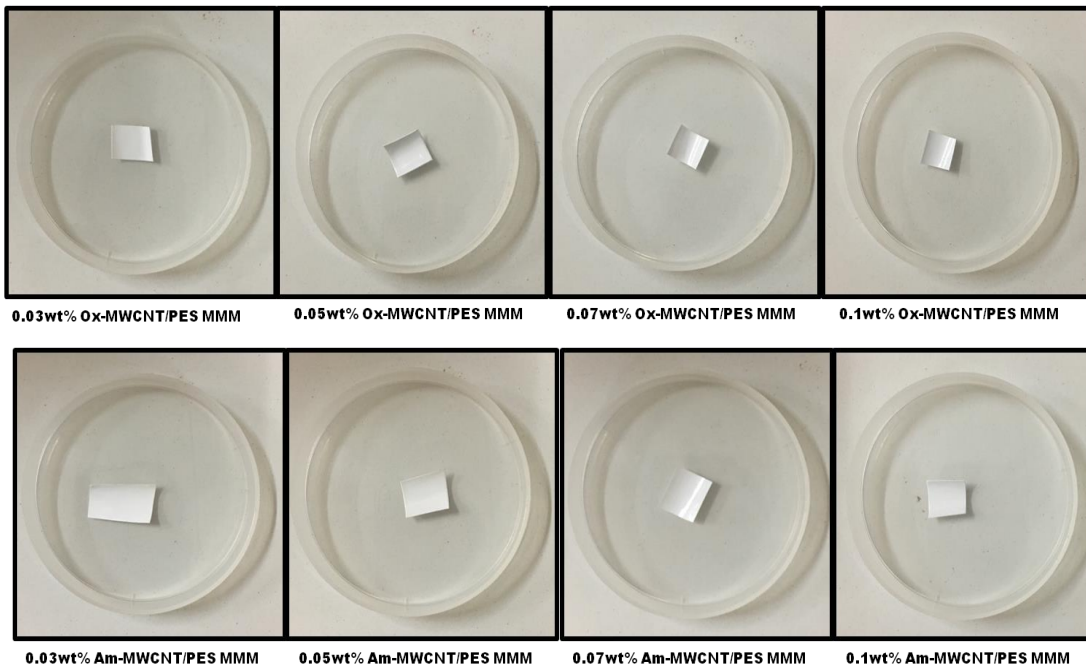


Figure 3.3 Images of prepared pristine PES and 1wt % f-MWCNT/PES mixed matrix membranes



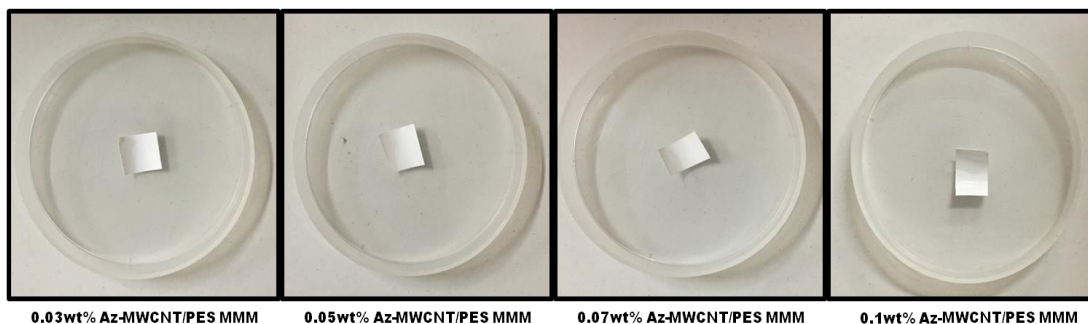


Figure 3.4 Images of prepared f-MWCNT/PES mixed matrix membranes having lower percentage of nanotubes

3.3. Sulfonation of polyether sulfone

Polyether sulfone was sulfonated using chlorosulfonic acid (Figure 3.5). In a typical procedure 20 g of PES was dissolved in 400 g of dichloromethane in a round bottom flask, with stirring at room temperature under inert atmosphere. Subsequently, 15-25 cm³ of chlorosulfonic acid was drop wise and slowly added to the reaction vessel using addition funnel. The reaction continued for 240 min and then was stopped by drop wise addition of reaction mixture into cold water to get the product. The white precipitates were filtered and washed with deionized (DI) water until the pH became approximately 5-6. Finally, the product dried at 100 °C for 24 h under vacuum. The resulting polymer was used for preparing mixed matrix membranes using functionalized MWCNTs as filler.

Chapter 3: Experimental route

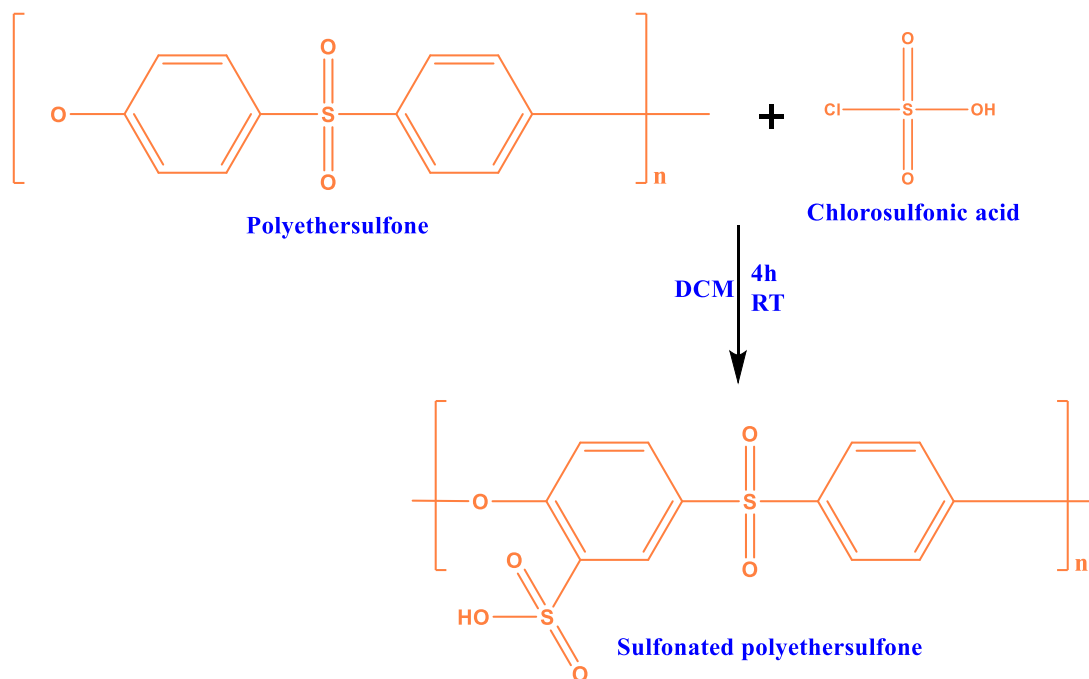


Figure 3.5 Schematic representations for the sulfonation of polyether sulfone

3.3.1. Incorporation of f-MWCNT into sulfonated polyethersulfone to form mixed matrix membranes

The sulfonated PES (SPES) was dissolved in N-methyl pyrrolidone to prepare the membrane dope solution and kept under stirring for 24 h for homogeneous solution. Various wt % of f-MWCNTs were added to the polymer dope solution followed by sonication for 48 h to ensure well dispersion of nanotubes. The composition of membranes is summarized in Table 3.1. The flat sheet membranes were prepared by phase inversion process using DI water containing 1% isopropanol as coagulation bath. The membranes were dried under vacuum at 80 °C and kept in DI water for further testing.

Chapter 3: Experimental route

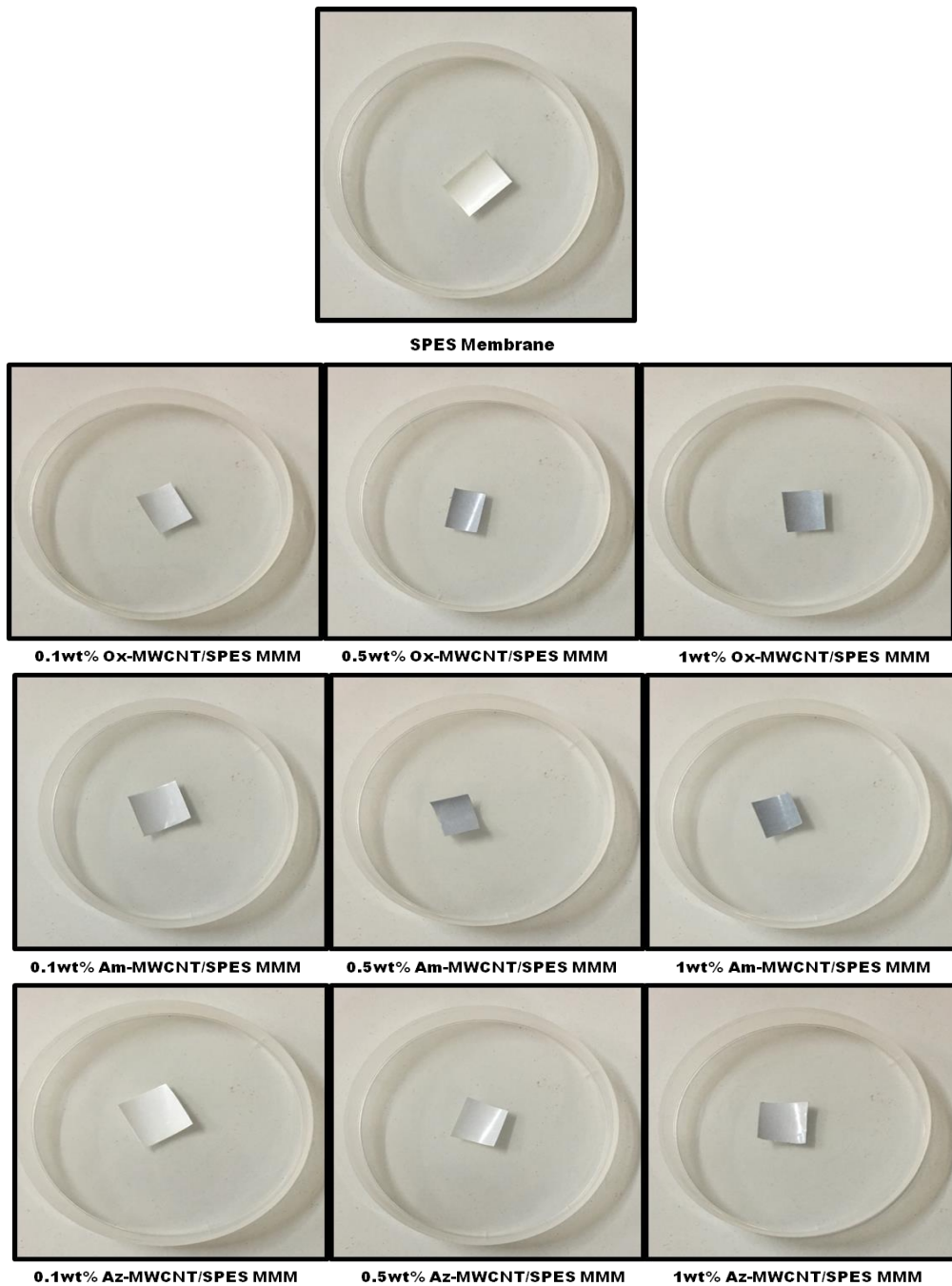


Figure 3.6 Images of prepared pristine SPES and f-MWCNT/SPES mixed matrix membranes

Chapter 3: Experimental route

3.4. Click coupling of Az-MWCNT/PES membrane

Coupling of azide moiety containing nanotubes with 1-pentyne was carried out via Cu(I) catalyzed click reaction. A mixed matrix membrane piece (10 X 5 cm size) containing azide functionalized nanotubes was immersed in de-ionized water in a 500 ml flask kept under inert atmosphere. CuBr(I) was added to the reaction flask when the mixture were light yellow. 1-Pentyne was added drop wise to the reaction flask under stirring and the reaction continued for 3 h to facilitate the complete conversion of azide group to 1,2,3 triazole ring. At this stage the solution turned green indicating the conversion of the Cu(I) to Cu(II). The contents were drained and the membrane was washed thoroughly with de-ionized water to remove excess of catalyst and dried under vacuum at 80 °C temperature for 8 h. The reaction scheme and picture of the membranes are shown in Figure 3.7 and 3.8 respectively.

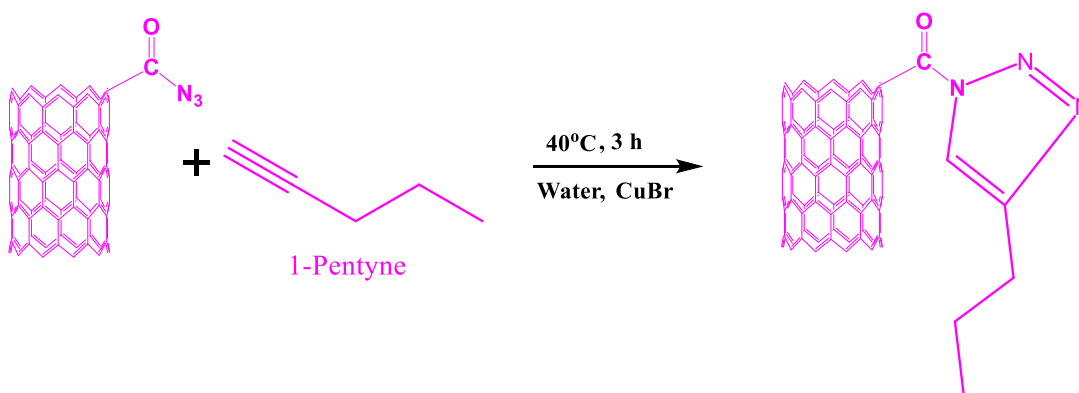


Figure 3.7 Reaction scheme of click reaction performed on the surface of the mixed matrix membrane

Chapter 3: Experimental route

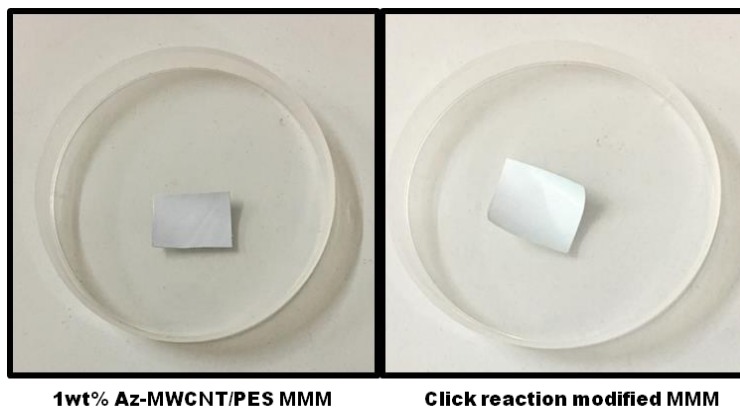


Figure 3.8 Images of click reaction modified and unmodified membranes

Table 3.1 Composition of membranes

Sr. No.	Code	Polymer	PES wt%	f-MWCNT wt%	Functional group of MWCNT
1.	M1	PES	18	0	-
2.	M2003	PES	18	0.03	Oxidized
3.	M2005	PES	18	0.05	Oxidized
4.	M2007	PES	18	0.07	Oxidized
5.	M201	PES	18	0.1	Oxidized
6.	M21	PES	18	1	Oxidized
7.	M3003	PES	18	0.03	Amide
8.	M3005	PES	18	0.05	Amide
9.	M3007	PES	18	0.07	Amide

Chapter 3: Experimental route

10.	M301	PES	18	0.1	Amide
11.	M31	PES	18	1	Amide
12.	M4003	PES	18	0.03	Azide
13.	M4005	PES	18	0.05	Azide
14.	M4007	PES	18	0.07	Azide
15.	M401	PES	18	0.1	Azide
16.	M41	PES	18	1	Azide
17.	S1	SPES	18	0	-
18.	S201	SPES	18	0.1	Oxidized
19.	S205	SPES	18	0.5	Oxidized
20.	S21	SPES	18	1	Oxidized
21.	S301	SPES	18	0.1	Amide
22.	S305	SPES	18	0.5	Amide
23.	S31	SPES	18	1	Amide
24.	S401	SPES	18	0.1	Azide
25.	S405	SPES	18	0.5	Azide
26.	S41	SPES	18	1	Azide
27.	C3	PES	18	1	Azide

Chapter 3: Experimental route

3.5. Characterization

3.5.1. Characterization of f-MWCNT

Functionalization of nanotubes and SPES were ensured by Fourier Transform Infrared Spectroscopy (FTIR), thermal stability was measured by thermo gravimetric analysis (TGA), and morphology was analyzed by Field Emission Scanning Electron Microscopy (FESEM).

3.5.2. Characterization of mixed matrix membranes

Membranes were analyzed with FESEM to characterize surface and cross section, Contact angle meter utilized to measure surface hydrophilicity of the membranes. TGA was used to analyze thermal stability, capillary flow porometer was used to measure porosity and pore dimensions, small angle neutron scattering (SANS) technique was applied to explore the arrangement of the pores within the membrane as well as the pore dimensions. Impedance analyzer measured the conducting nature of the membranes. Atomic Force Microscopy (AFM) has given the roughness parameters of the membrane surface. X-ray Photoelectron Spectroscopy confirmed the click modification of the membranes. Mechanical properties of the membranes were measured on Tensile testing machine.

3.5.3. Fourier Transform Infrared Spectroscopy (FTIR):

FTIR Shimadzu 8400S spectrophotometer was used to detect functional group associated with nanotubes.

3.5.4. Thermo gravimetric Analysis (TGA):

TGA-50 Shimadzu was used to measure thermal behaviour of f-MWCNT and membranes.

Chapter 3: Experimental route

3.5.5. Field Emission Scanning Electron Microscopy(FESEM):

Morphology of the f-MWCNT and membranes were studied by FESEM (JSM-7100F JEOL) and FEG-SEM 450. FESEM analysis was performed at Central Salt and Marine Research Institute, Bhavnagar and SICART, V.V. Nagar.

3.5.6. Atomic Force Microscopy (AFM):

The Atomic Force Microscopy device was NT-MD-INTEGRA 2005, equipped with Nova 1.0.26.1424 software, utilized to further probe the surface profile of membrane samples in semi contact mode. Silicon nitride was used as probe with reflective side as gold. The instrument consists of cantilever/tip assembly that interacts with the samples which is known as AFM probe. AFM probe interacts with the sample through a raster scanning motion. The movement of AFM tip was monitored through a laser beam reflected off the cantilever. Position sensitive photo detector was used to track the reflected laser beam.

3.5.7. Zeta potential:

Zeta potential is a measure of electrokinetic potential denoted by Greek letter zeta (ζ). The streaming potential E is used to determine the membrane zeta potential by using the Helmholtz-Smoluchowski equation [221]

$$\zeta = \frac{\Delta E \eta \lambda}{\epsilon \Delta P}$$

Where ΔP is the pressure drop across the pore channels, η is the solution viscosity, λ is the solution conductivity and ϵ is the dielectric constant of the electrolyte solution. Generally the separation performance of the membranes were described in terms of size exclusion mechanism but in some cases the property of electrical double layer near the pore walls is an essential factor of the pore

Chapter 3: Experimental route

volume. When an electrolyte solution is passed through a capillary under certain pressure an electrical potential is produced which is known as streaming potential. The charge related modification on the surface or inside the pores of the membranes are observed by the evaluation of streaming potential [222].

Stern has introduced the model of electrical double layer in 1994 with the combination of the Helmholtz and Gouy Chapman models. The layer at distance of about one molecule is known as Stern layer. In this layer, the oppositely charged ions can reduce the surface potential linearly. Moreover, there exists another layer which includes other scattered ions. Here the reduction in potential is not linear but approaches to zero, this implies that ion concentration is inversely proportional to the distance.

Polymeric membranes carry surface charge due to the presence of functional group on surface. These membranes in contact with the aqueous solution, forms electrical double layer, due to the compensation of the surface charge of membranes with the counter ions in the solution near the surface. The characteristic of electrical double layer is that surface charge is balanced by counter ions, some of these counter ions are situated very close to surface in the Stern layer and remaining are distributed at some distance from the surface in the Diffuse layer. The potential at the boundary between Stern and Diffuse layer is known as Stern potential, which cannot be measured directly. However, zeta potential is often considered as a satisfactory alternate for stern potential. The potential at the plane of shear between the solid surface and solution where the comparative movement occurs between them is zeta potential [223]. There are four basic kinds of electro kinetic effects which can be used to evaluate zeta potential according to the given conditions. These are Electrophoresis, Electro-osmosis, Sedimentation potential and Streaming potential. The streaming potential technique is most appropriate for membranes.

Chapter 3: Experimental route

3.5.8. Contact angle meter:

Water contact angle of the membrane surface was measured by contact angle meter ACAMNSC 03, M/s Apex Instruments Pvt. Ltd. to measure hydrophilicity of membranes. One drop of De-ionized water was taken onto membrane surface with the help of syringe and contact angle measured immediately. An average of seven readings was taken for each membrane.

3.5.9. Capillary flow porometry:

The morphology of the membrane was also analyzed by Capillary flow porometer (Porous Materials Inc., USA Model 1100 AEX) at Smita Labs, IIT Delhi. It is an expulsion method where we have considered pores of the membrane as capillary. Wetting fluid used for soaking the membrane is Galwick. The surface tension (γ) of the fluid is 1.59 N/m² which makes zero contact angles with the membrane surface. So the membrane sample wets perfectly so that all the pores were filled with the wetting fluid. Then the gas was passed through the samples and pressure applied and increases gradually till all the fluid was removed from the pores. And gas was allowed to pass through the pores. Larger pores are emptied first followed by the smaller pores. The pressure at which the largest pore emptied and the gas pass through them is called bubble point pressure. Keep on increasing the pressure smaller pores were also emptied and gas pass through the pores. Washburn equation which converts the applied pressure into pore diameter was used to calculate the pore characteristic of the sample.

$$D=4\gamma \text{ Cos } \theta / P \quad (1)$$

Where P is the differential pressure, γ is surface tension θ is contact angle and D is diameter of the pore. In this case contact angle is zero so we get modified equation from which we calculate the pore diameter.

Chapter 3: Experimental route

$$D=4\gamma / P \quad (2)$$

3.5.10. Small angle neutron scattering (SANS):

The small angle neutron scattering (SANS) experiments were performed on SANS Diffractometer at Dhruva Reactor, Mumbai, India [224]. The instrument utilizes a neutron velocity selector to get a monochromated neutron beam with a mean wavelength of 5.2 Å, with a wavelength resolution ($\Delta\lambda/\lambda$) of approximately 15%. The angular divergence of the incident beam was $\pm 0.5^\circ$. The scattered neutrons were detected using a linear He³ position sensitive gas detector. The data were collected over the wave vector range ($Q = 4\pi\sin\theta/\lambda$) of 0.015 – 0.35 Å⁻¹, where 2θ is the scattering angle and λ is the wavelength of incident neutrons. The diffractometer is well suited for the study of a wide variety of system having characteristic dimensions between 10 – 300 Å. The membrane samples was cut into small pieces of 1 X 1.5 cm² dimension and few pieces were put together in the aluminium foil and positioned in the path of the beam. The data analysis was done after the data were corrected for the direct beam and the background contribution.

3.5.11. Impedance Measurement:

The conducting property of the polymeric mixed matrix membranes has been measured on Precision LCR Meter AGILENT E4980A within the frequency range 20 Hz to 2 MHz at Department of Physics, Faculty of Science, The M. S. University of Baroda. The membrane was placed between the two sliver electrodes having 0.885 cm² area. The experiment was performed on varying voltages. The ac conductivity (σ) of the

Chapter 3: Experimental route

membrane was calculated from the impedance data in Siemens per cm unit from the following equation

$$\sigma = \frac{1}{r_b} \times \frac{t}{A} \quad (3)$$

Where r_b is impedance value obtained from the data. A is area of the silver electrodes between which membrane should fixed and t is the thickness of the membrane.

3.5.12. X-ray photoelectron spectroscopy (XPS):

XPS is a surface sensitive quantitative spectroscopic technique which measures the elemental composition. XPS spectra are essentially obtained by irradiating a material with a beam of X-rays while simultaneously measuring the kinetic energy and number of electrons by the detector, that escape from the samples being analyzed.

3.5.13. Tensile test:

Tensile test in dry state at room temperature using Lloyd LRX instrument at a speed of 2 mm min⁻¹ and gauge length 14 mm was carried out. Membrane stripes of 5 cm long and thickness 0.12 - 0.23 mm were taken for the analysis.

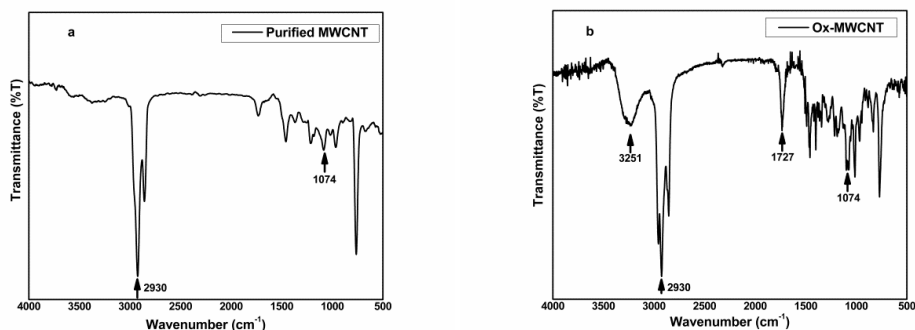
3.6. Characterization of functionalized MWCNT:

3.6.1. FTIR

The FTIR spectra of purified, oxidized, amide and azide functionalized MWCNTs confirms that these functionalities have successfully been attached to the nanotubes (Figure 3.9). In the purified MWCNT, the band at 2930 cm⁻¹ is due the carbon bonded to hydrogen and 1074 cm⁻¹ corresponds to the

Chapter 3: Experimental route

aromatic C=C stretching vibrations in the graphene structure of CNT [225]. The spectra of carboxylic nanotubes shown band at 3251 cm^{-1} which is attributed to the O-H stretch from carboxyl group (O=C-OH and C-OH). The peak at 1727 cm^{-1} is associated with C=O stretch of COOH group at oxidized nanotubes. Band at 1064 cm^{-1} revealed the presence of aromatic C=C stretching vibrations in the graphene structure of MWCNT [225]. This confirmed the carboxylic functionalization of nanotubes. The amide functionalized MWCNT spectra showed disappearance of the peak at 1727 cm^{-1} and analogous emergence of band at lower frequency (1662 cm^{-1}) designated to the amide carbonyl stretching vibrations. The band appeared at 3490 cm^{-1} corresponds to the presence of N-H stretching vibrations. Further, existence of bands at 1573 cm^{-1} and 1223 cm^{-1} are attributed to the presence of -N-H in plane and C-H stretching vibrations, which further authenticate the presence of amide functional group at nanotube. For azide functionalized nanotubes sample, the new band appeared 2304 cm^{-1} which confirmed N=N stretching vibrations of azide moiety.



Chapter 3: Experimental route

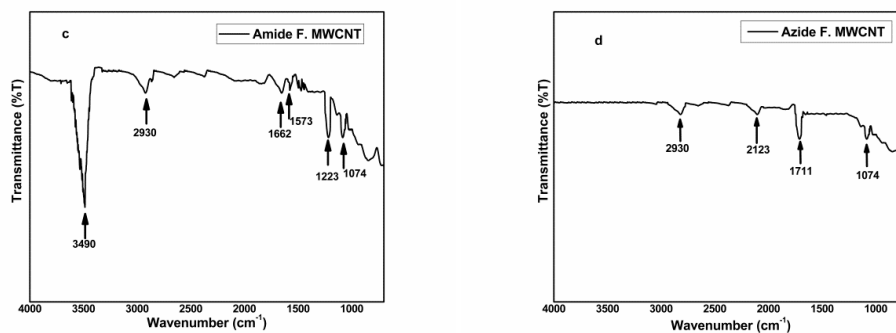


Figure 3.9 FTIR spectra of purified MWCNT(a) oxidized MWCNT(b) amide functionalized MWCNT(c) azide functionalized MWCNT(d)

3.6.2 TGA

From the TGA study of purified CNT, oxidized, azide and amide functionalized CNT we have concluded that thermal stability of MWCNT decreases after functionalization (Figure 3.10). Azide functionalized CNTs were having least thermal stability among all the three functionality.

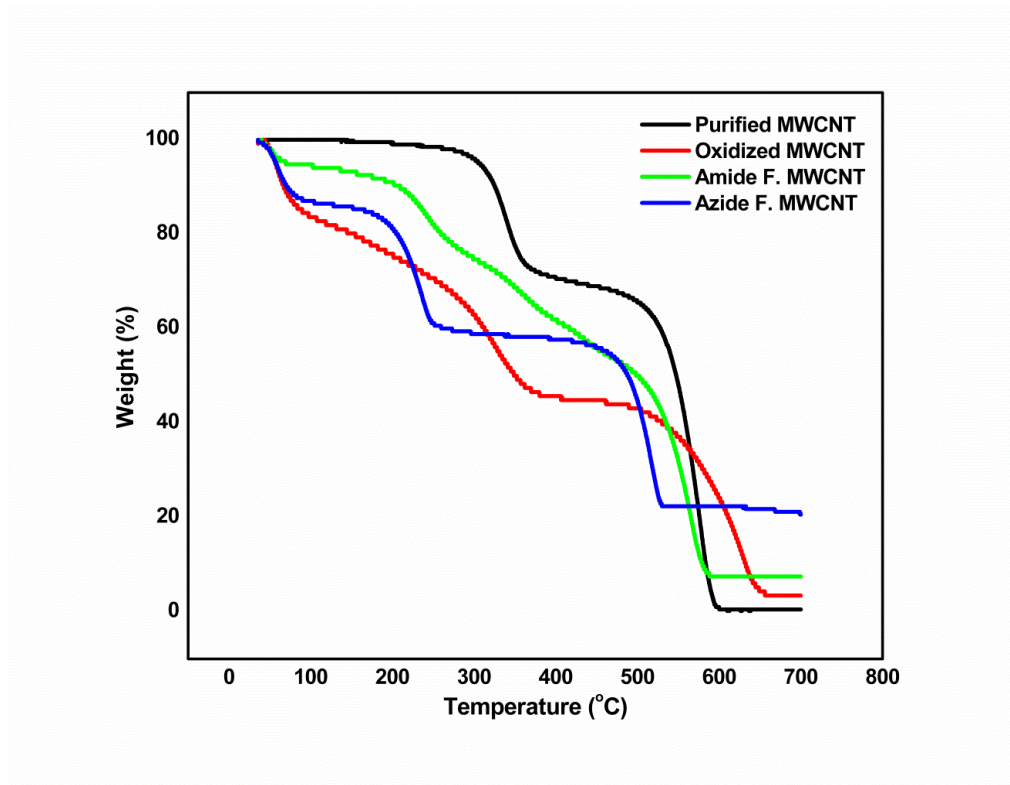


Figure 3.10 TGA spectra of functionalized multiwalled carbon nanotubes

3.6.3 Field emission Scanning electron microscopy

The micrographs obtained from the FESEM analysis of functionalized CNT showed that the morphology of the membranes not differ significantly for dissimilar functionalities (Figure 3.11).

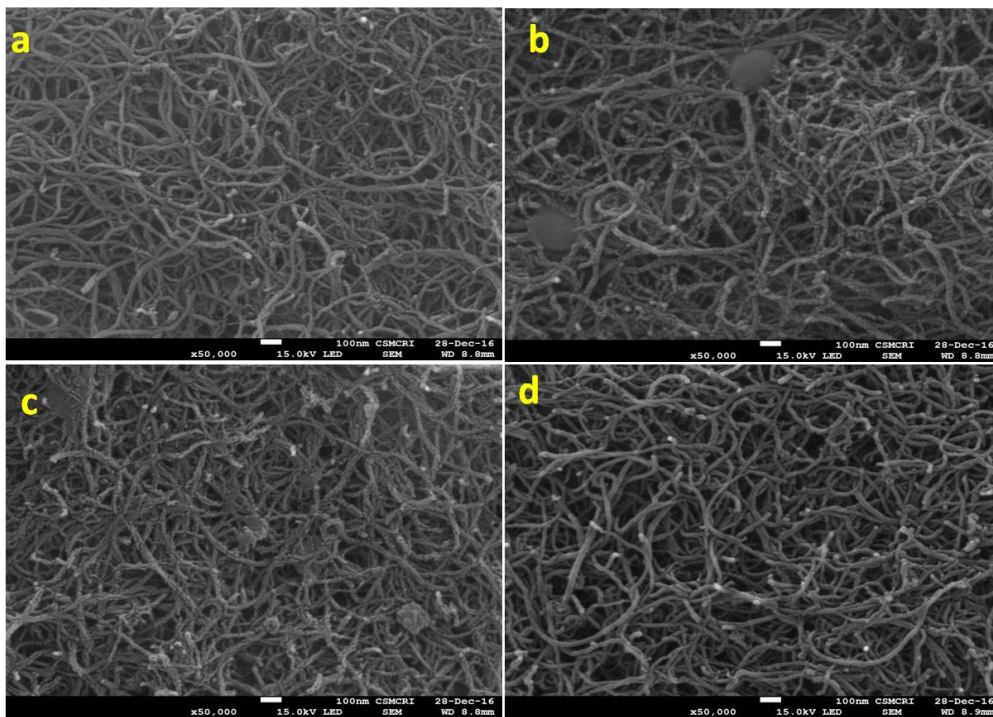


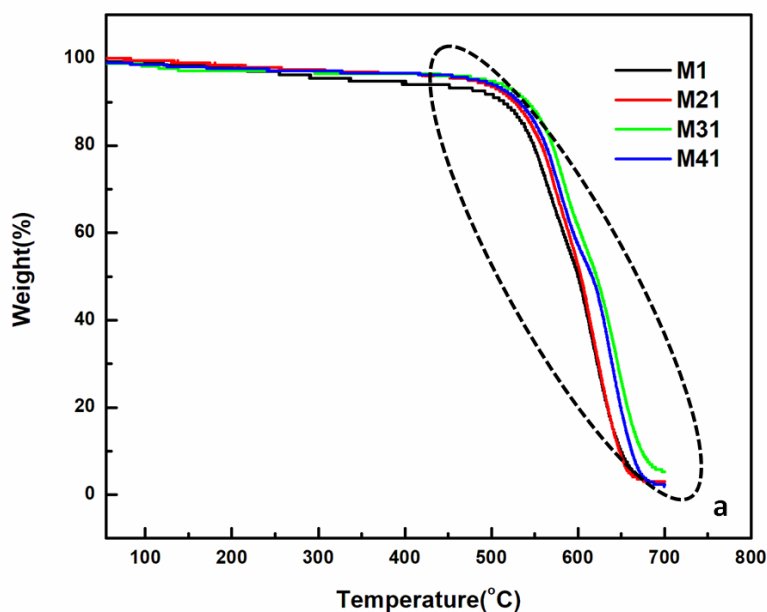
Figure 3.11 FE-SEM micrographs of functionalized MWCNT (a) Oxidized [C1] (b) Acylated [C2] (c) Azide functionalized [C3] (d) Amide functionalized [C4]

Chapter 3: Experimental route

3.7 Thermal, mechanical and electrical characterization of f-MWCNT/PES mixed matrix membranes

3.7.1 TGA of membranes

The TGA of the pristine as well as MWCNT incorporated membranes were taken to observe the thermal stability of the membranes (Figure 3.12). It was found that thermal stability of mixed matrix membranes was not adversely affected due to the presence of the functionalized nanotubes and in fact there was a marginal increase in the stability. For example at 550 °C the M1 is degraded by 21% whereas the other membranes M21, M31, M41 all degrade only 17% at the same temperature.



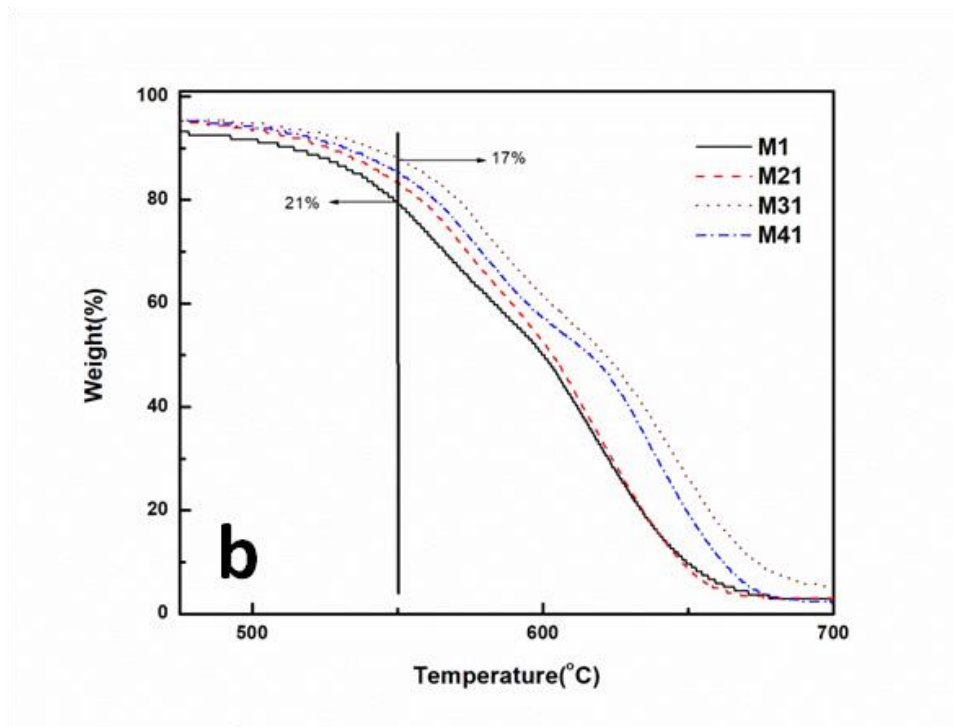


Figure 3.12 Thermal stability of mixed matrix membranes as measured by TGA (b) Enlarged image

3.7.2 Tensile strength

Tensile properties of membranes revealed that pristine PES membrane was able to withstand elongation at break up till 11.3%. The maximum yield stress this membrane could withstand until 4.4 MPa. The stress-strain curve of PES and f-MWCNT/PES mixed matrix membranes are demonstrated in Figure 3.13 and 3.14. The excellent bonding strength between PES and functionalized MWCNTs has together provided improvement in the mechanical properties of the membrane. It is observed that when the oxidized nanotubes were dispersed in the PES matrix the capacity to withstand higher stress improved to 97.4 % and for amide and azide functionalized MWCNT incorporated membranes, it was improved to 98.05 and 98.1% respectively. The 1wt % Az-MWCNT/PES

Chapter 3: Experimental route

mixed matrix membrane was having improved maximum yield stress withstanding capacity of 5.9 MPa. In conclusion, azide functionalized MWCNT are showing improved mechanical properties than pristine PES membrane.

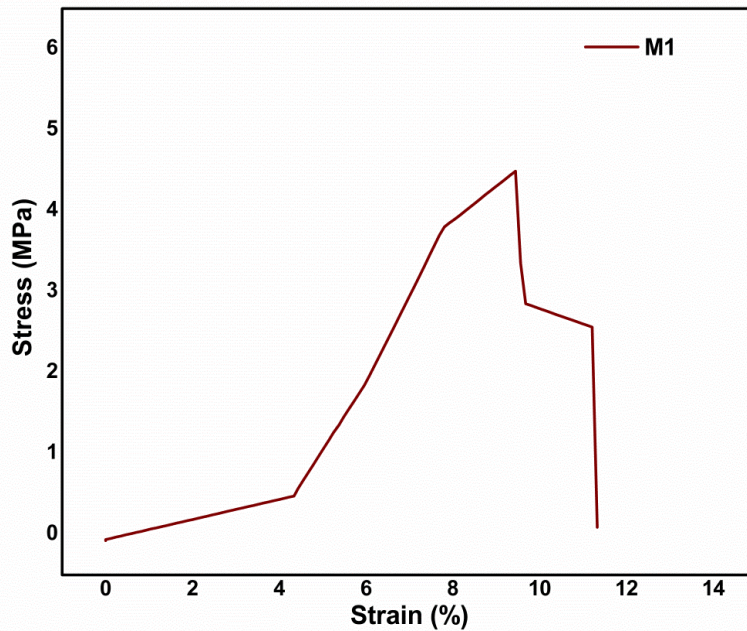


Figure 3.13 Stress vs Strain curve of pristine PES membrane [M1]

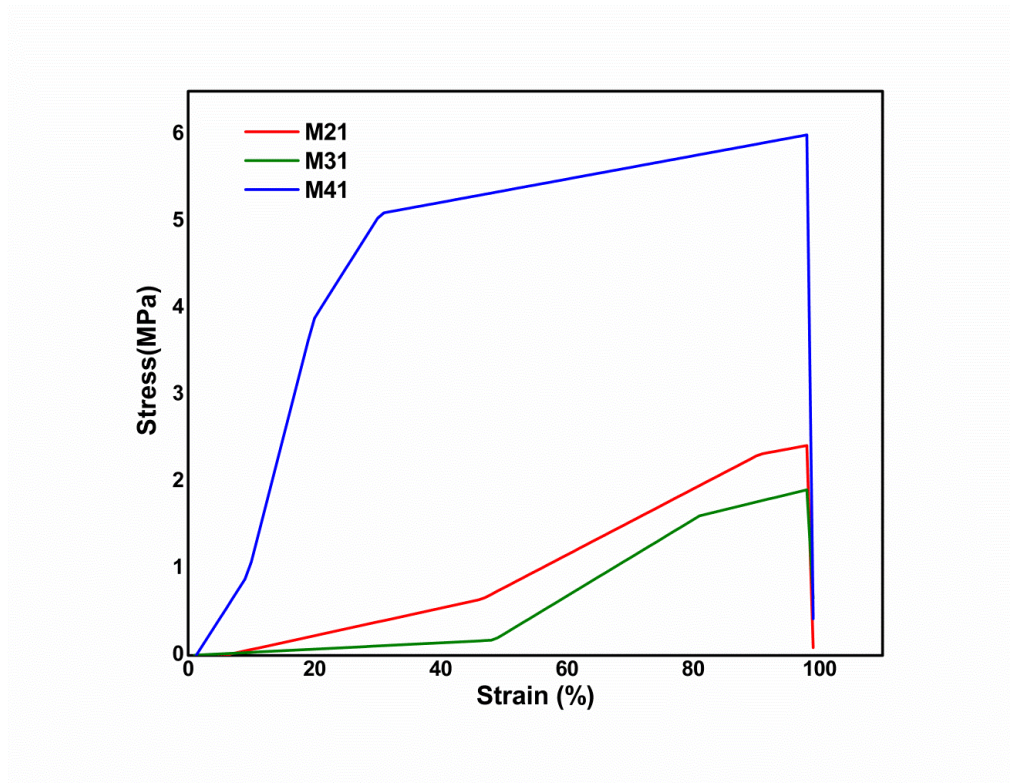


Figure 3.14 Stress vs strain curve of 1wt% Ox-MWCNT/PES [M21], 1wt% Am-MWCNT/PES [M31], 1wt% Az-MWCNT/PES [M41] membranes

3.7.3 Electrochemical Impedance Analyzer

A small piece of membrane was characterized by the electrochemical impedance analyzer. Pristine PES membrane and functionalized MWCNT mixed matrix membrane was analyzed by the LCR meter. In the case of pristine membrane, we have observed nearly constant phase angle so we were not getting ac conductivity. This observation may be attributed to the solid packed structure of PES and no filler or charge carrier in the polymer structure which could result into transport or conduction process. Therefore no ac conductivity was observed. However it may provide high dc conductivity or insulating character. While in the case of mixed matrix membranes which

Chapter 3: Experimental route

contains functionalized MWCNT as filler material, Z' (real impedance) was plotted against Z'' (imaginary impedance) which gives a semicircle curve (Figure 3.15). Such semicircle attributed to the parallel combination of bulk resistance and capacitance of the mixed matrix film. When this film was subjected to variation of temperatures, no change in bulk resistance was observed. But with the change of biasing voltage across the film starting from 400 mV to 900 mV, the bulk impedance of the film decreases maintaining the semicircle character. On increasing the voltage there was decrease in the impedance value hence increase in the conductivity. The conductivity values have shown in Table 3.2.

Table 3.2. Conductivity of mixed matrix membrane (M41) at different voltages

Sr. No.	Voltage (mV)	Conductivity (S/cm)
1	400	1.84×10^{-8}
2	500	2.17×10^{-8}
3	600	2.96×10^{-8}
4	700	3.59×10^{-8}
5	800	5.70×10^{-8}

Conductivity was changing because of the release of the trapped electrons between the MWCNT. When the voltage was increased, more trapped electrons were released to provide the lower resistance/impedance. This confirmed the presence of functionalized MWCNT in the polymer matrix of the membrane and this also showed the successful functionalization of the MWCNT. Thus we may conclude that the mixed matrix membrane is thermally insulating while electrically conducting.

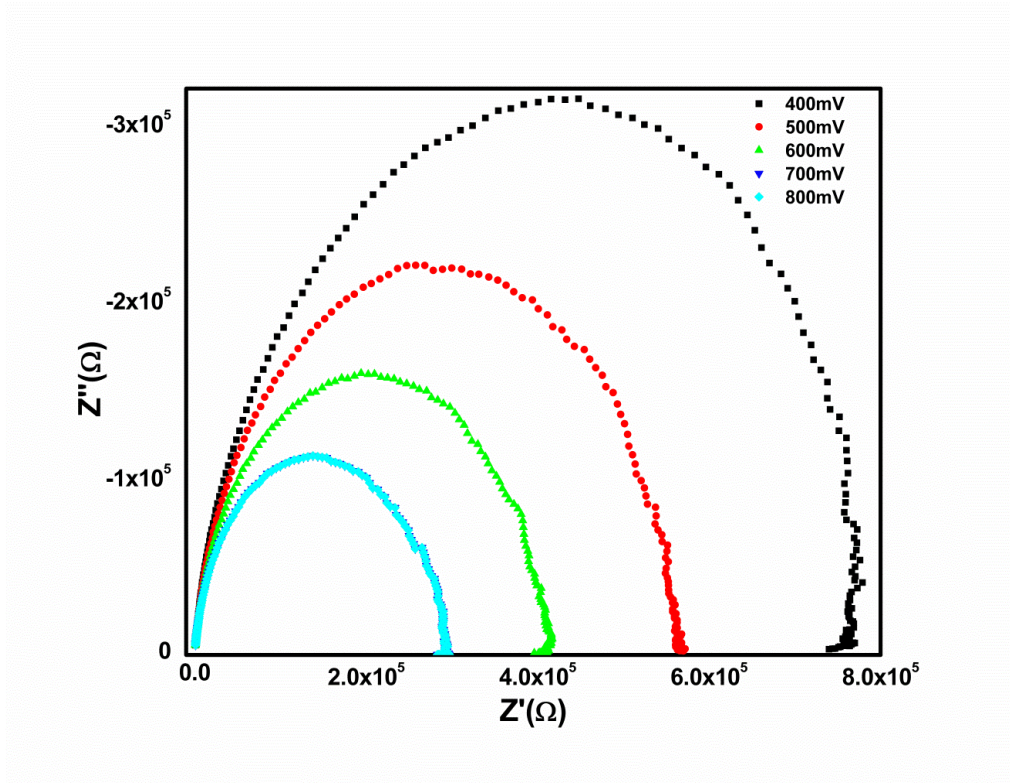


Figure 3.15 Impedance spectra of Az-MWCNT/PES mixed matrix membrane

Chapter 3: Experimental route

3.8 Characterization of sulfonated polyether sulfone

3.8.1 FTIR

The substitution of SO_3H group to the polyethersulfone was confirmed by FTIR analysis. On comparing the FTIR spectra of SPES and PES shown in Figure 3.16, the appearance of band at 3444 cm^{-1} in SPES spectra was attributed to the stretching of hydroxyls of sulfonic acid groups and the absorption peak appeared at 1027 cm^{-1} was the characteristic of aromatic SO_3H symmetric stretching vibrations [226]. Other signals were common in both spectra, signals at 1327 cm^{-1} and 1297 cm^{-1} are due to asymmetric $\text{O}=\text{S}=\text{O}$ stretching of sulfone group; peak at 1247 cm^{-1} corresponds to asymmetric $\text{O}-\text{C}-\text{O}$ stretching of aryl ether group; signal at 1148 cm^{-1} was for symmetric stretching of sulfone group; signals at 1107 cm^{-1} and 1072 cm^{-1} were for aromatic ring vibrations; at 1077 cm^{-1} signal for vibrations of aromatic ring bonded to sulfonate group appears [227-229]. This gives the authentication of attachment of sulfonic acid group to the polymer chain.

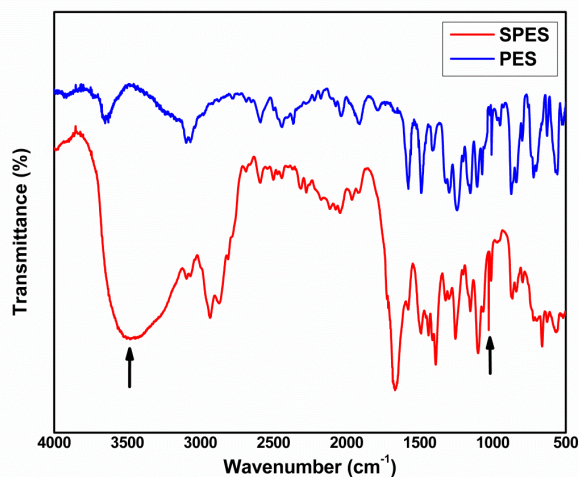


Figure 3.16 FTIR spectra of polyethersulfone (PES) and sulfonated polyethersulfone (SPES)

Chapter 3: Experimental route

3.8.2. Nuclear magnetic resonance (NMR) spectroscopy

3.8.2.1. H^1 NMR

The substitution of sulfonic acid group to the benzene ring of polyethersulfone was confirmed by NMR spectroscopy. As can be seen from the H^1 NMR spectra a significant downfield shift 7.2 to 8.3 ppm of the hydrogen marked as H_d at the aromatic ring in the SPES structure (Figure 3.17) occurs due to the presence of sulfonic acid group which was in agreement with previously reported studies [230-233].

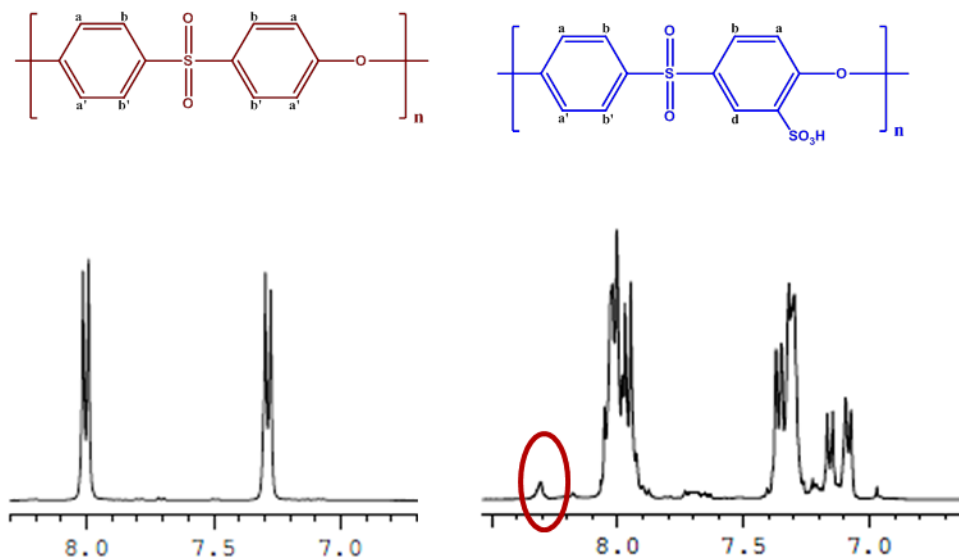


Figure 3.17 1H NMR spectra of PES and SPES polymer

Chapter 3: Experimental route

3.8.2.2. C13 NMR

In the C13 NMR spectra of SPES (Figure 3.18, 3.19), some additional signals were present which was present due to the sulfonic acid bonded to the benzene rings influencing the chemical shifts of neighboring carbon atoms, compared to the C13 spectra of PES [234].

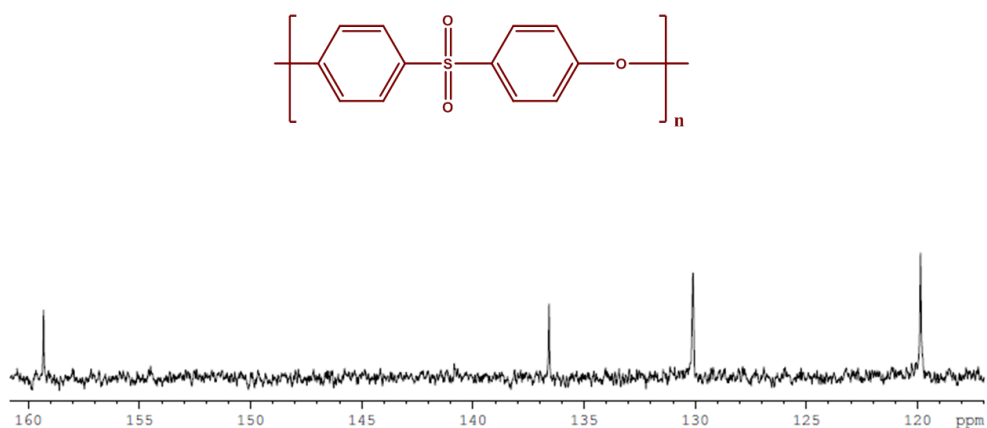


Figure 3.18 C13 NMR spectra of Polyethersulfone polymer

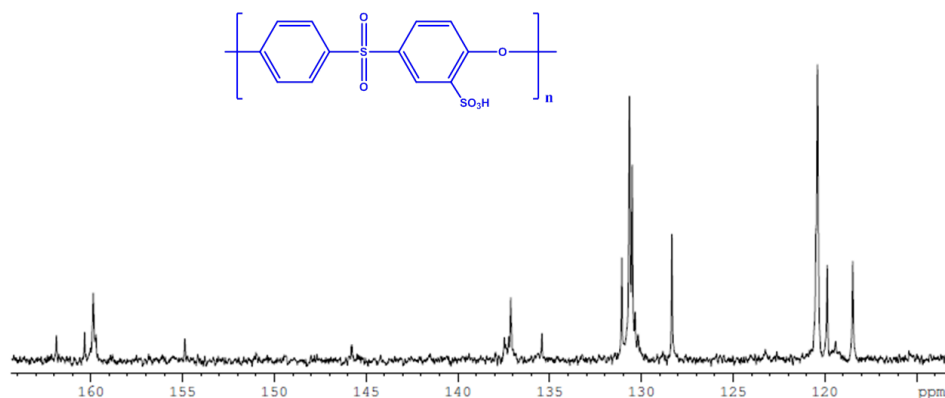


Figure 3.19 ¹³C NMR spectra of sulfonated polyether sulfone polymer

3.8.3. TGA

The thermal stability of SPES was determined by thermo gravimetric analysis. In the SPES sample decomposition at three different temperature ranges can be seen in the Figure 3.20. First decomposition occurred at around 100 °C, which is related to the loss of water bonded to sulfonic acid group. The second degradation takes place at around 400 °C, which is due to decomposition of sulfonic acid groups. The third decomposition at around 480 °C is attributed to the degradation of polymer main chain. However, PES polymer shows only one sharp degradation at around 540 °C, which is assigned to the polymer main chain degradation. In addition, the lower thermal stability of SPES could be due to the enhanced asymmetry in PES structure which is attributed to the addition of sulfonic acid group that makes it less regular hence less stable [235-236].

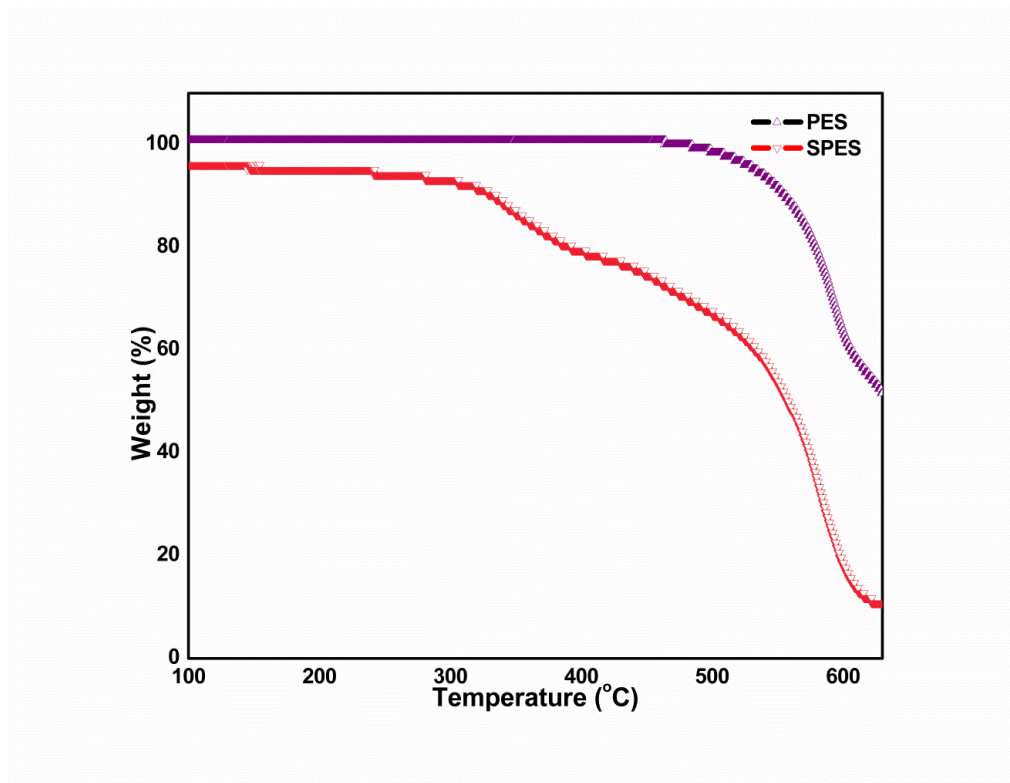


Figure 3.20 TGA spectra of polyether sulfone and sulfonated polyethersulfone

3.8.4. Viscosity measurement and degree of sulfonation

Viscosity study has been performed to perceive probable chain scission during the sulfonation process. As shown in Table 3.3, the sulfonated polyethersulfone had inherent viscosity value equal to 1.84 dL/g which were greater than the parent polyethersulfone. These results indicated that there is no chain cleavage or degradation of original polymer due to sulfonating agent [237]. The intrinsic viscosity of SPES sample had increased compared to the value for PES, possibly due to the enhancement of interchain interactions which results higher resistance

Chapter 3: Experimental route

to the stretching of the main chains because of the attachment of SO₃H group [238]. The degree of sulfonation obtained for SPES sample was 30.22%.

Table 3.3 Viscosity values for polyethersulfone and sulfonated polyethersulfone in solvent NMP at 30°C

	η_{rel}	η_{sp}	η_{red}	η_{inh}	η_{int}
PES	2.21	1.12	2.25	1.50	1.72
SPES	2.24	1.24	2.49	1.61	1.84

3.8.5. X-Ray Diffraction (XRD)

The X-Ray diffraction analysis has been performed to evaluate the structural aspect of the post sulfonation polymer. The data of XRD analysis of polyethersulfone (PES) and sulfonated polyethersulfone (SPES) is summarized in Table 3.4. Both the polyethersulfone and sulfonated polyethersulfone have showed characteristic of amorphous polymer [239]. The data were compared in terms of peak position, peak intensity and d-spacing. The peak intensity was decreased in SPES compared to PES which implies reduced macromolecular orientation within the polymer.

Table 3.4 X-Ray diffraction values of PES and SPES

	$2\theta(^{\circ})$	Peak Intensity (Counts per second)	d-spacing (\AA°)
PES	21.07	452.19	4.21
SPES	19.7	274	4.49

3.9 Thermal and mechanical characterization of SPES/f-MWCNT membranes

3.9.1 TGA

The TGA plots of SPES and SPES/f-MWCNT mixed matrix membranes showed three step weight degradation (Figure 3.21). The first weight loss was between 100 °C to 190 °C which was obviously ascribed to the loss of water attached to the hygroscopic sulfonic acid group. The second degradation was observed at around 300 °C which may be due to the decomposition of sulfonic acid group. The third weight loss was at around 500 °C which was attributed to the polymeric backbone degradation. The thermal stability of SPES membrane was improved with the addition of azide functionalized MWCNT fillers in different weight percentage [0.1 wt% (S401), 0.5 wt% (S405) and 1 wt% (S41)].

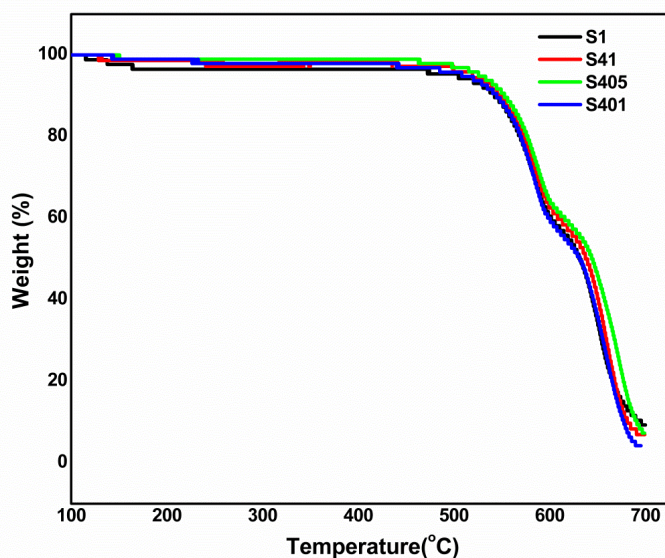


Figure 3.21 TGA curves of SPES membrane and 0.1 wt% Az-MWCNT/SPES(S401), 0.5 wt% Az-MWCNT/SPES(S405), 1 wt% Az-MWCNT/SPES(S41) mixed matrix membranes

Chapter 3: Experimental route

3.9.2 Tensile strength

The durability of the mixed matrix membrane widely gets affected by the mechanical failure [240]. The tensile properties of the membranes were evaluated by performing tensile strength test. The tensile strength was improved as compared to the bare SPES membrane. When using different functionalized nanotubes as fillers in the polymer matrix the tensile strength varies and the highest was in the case of azide functionalized MWCNT. Stress vs strain curve is shown in Figure 3.22.

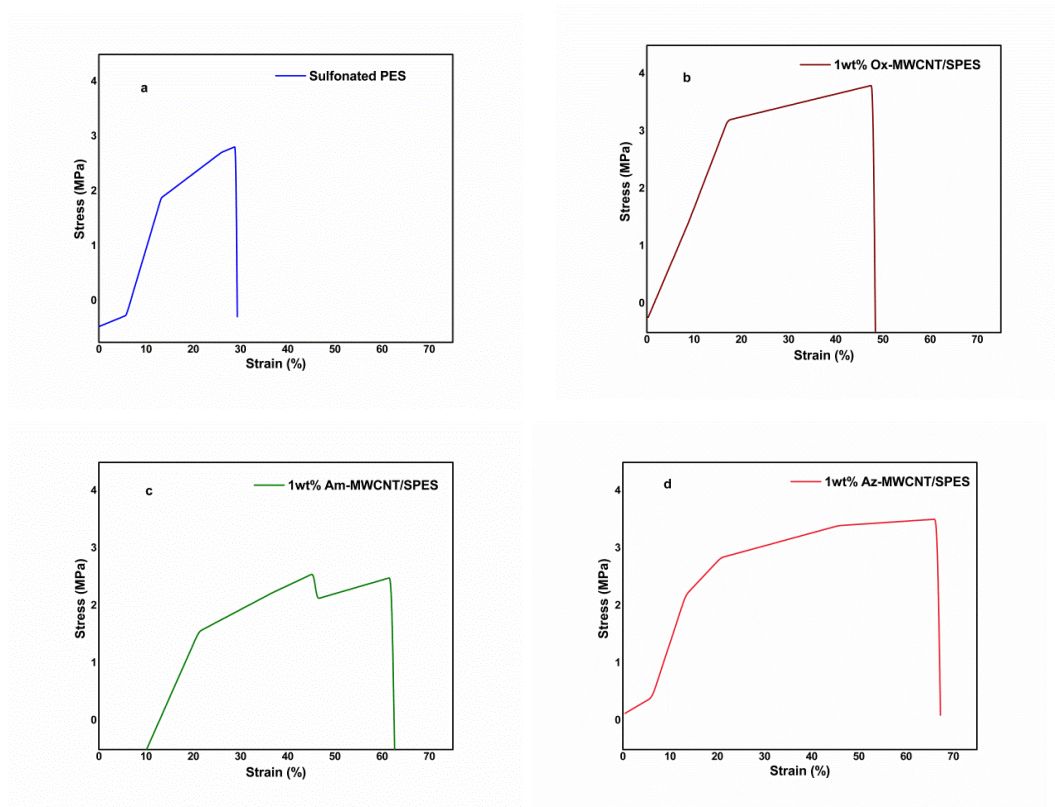


Figure 3.22 Stress vs strain curve of pristine SPES (a) 1wt% Ox-MWCNT/SPES (b) 1wt% Am-MWCNT/SPES (c) 1wt% Az-MWCNT/SPES membranes (d)

Chapter 3: Experimental route

The SPES, 1wt% Ox-MWCNT/SPES, 1wt% Am-MWCNT/SPES and 1wt% Az-MWCNT/SPES membrane samples can withstand elongation at break up till 28.7%, 47.5%, 61.75% and 65.9% respectively. The maximum stress that the membranes can withstand is 2.78 MPa for pristine sulfonated SPES, 3.78 MPa for oxidized, 2.46 MPa for amide and 3.48 MPa for azide membranes.

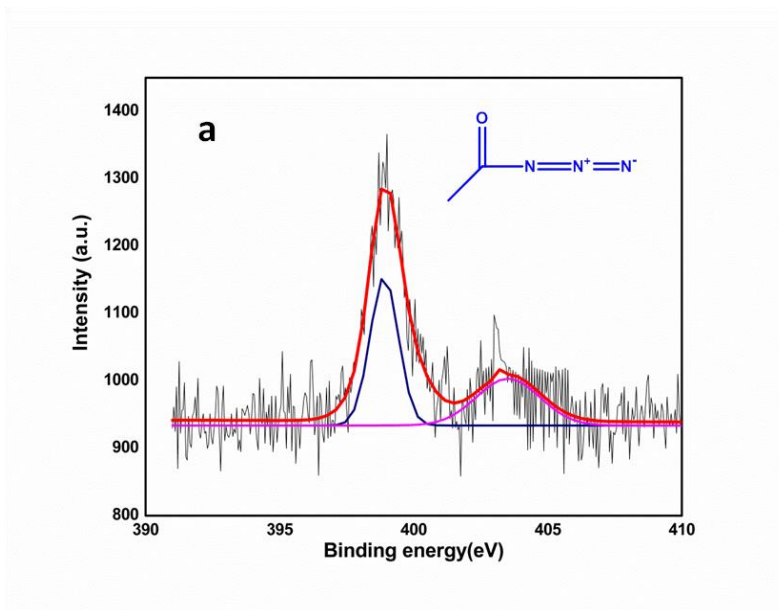
Chapter 3: Experimental route

3.10 Surface, thermal and mechanical characterization of click reaction modified PES/Az-MWCNT membranes

3.10.1 X-ray photo electron spectroscopy (XPS)

XPS is a surface sensitive quantitative spectroscopic technique that measures the elemental composition. XPS spectra are essentially obtained by irradiating a material with a beam of X-rays while simultaneously measuring the kinetic energy and number of electrons by the detector, that escape from the samples being analyzed. Both the unmodified and modified mixed matrix membrane was characterized by X-ray photo electron spectroscopy (XPS) to identify the surface group and to confirm the effective click coupling on the membrane surface.

X-ray photoelectron spectroscopy (XPS) was used to ensure the modification of membrane. XPS is an important technique for the surface characterization and analysis of polymers. It provides total elemental analysis except hydrogen and helium of any solid sample which is vacuum stable or can be made vacuum stable by cooling. Chemical bonding information is also provided [241]. Figure 3.23 shows the N1s XPS spectra of unmodified (a) and the modified (b) membrane.



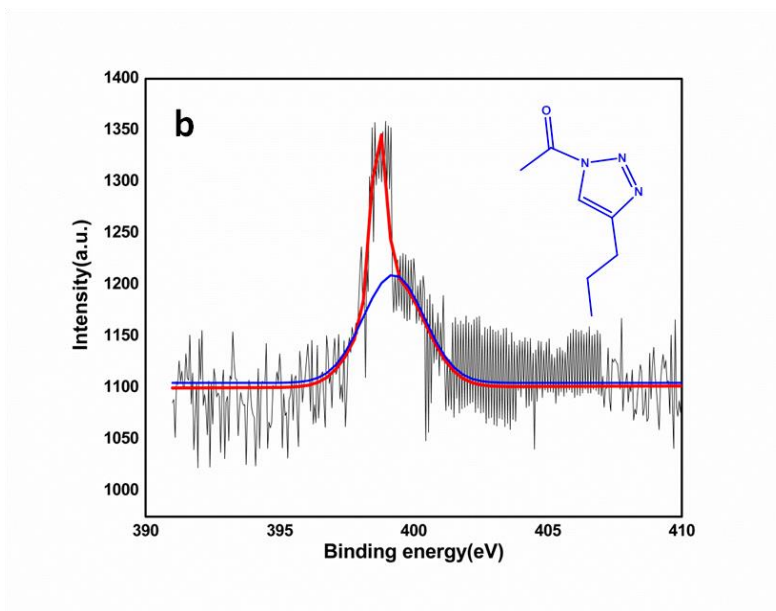


Figure 3.23 XPS spectra of (a) unmodified azide functionalized MWCNT membrane [M41] and (b) Alkyne treated membrane [C3]

In Figure 3.23a XPS N1s spectra of unmodified membrane, the peaks are at 399 eV and 403 eV with a peak area ratio of 2:1. In the azide group, the resonating structure can be shown as



In these two structures, the two terminal nitrogen are equivalent and so only two peaks are seen, one for the two terminal nitrogen and one for the central nitrogen with a ratio of 2:1. These peaks are due to the azide group ($-\text{N}=\text{N}^+=\text{N}^-$) present on the membrane surface and matches with the literature reported value [242].

Figure 3.23b shows the XPS N1s spectra of the surface after it undergoing click reaction in presence CuBr(I) catalyst. The absence of peak at 403 eV and

Chapter 3: Experimental route

broadening of the peak at 399 eV is consistent with the formation of 1, 2, 3, triazole, which indicates that the chemical environment of the three nitrogens is now different and so one of the peak at 403 eV vanishes and the broadening of the 399 eV peak takes place. The broad peak arising from the three nitrogens can further be resolved under stringent conditions which we did not perform. Nonetheless, the disappearance of the peak at 403 eV is consistent with that reported in literature [243] and sufficient to confirm that the click reaction was successfully carried out where the azide group was converted to a triazole ring, under the mentioned conditions.

3.10.2. TGA of membranes

Thermal stability of the modified membranes is analyzed by thermo gravimetric analysis. The decomposition temperature (T_d) for Azide functionalized MWCNT (M41) is 414°C while 464 °C is for click modified membrane. This is evident that the thermal stability of the modified membrane is improved significantly (Figure 3.24).

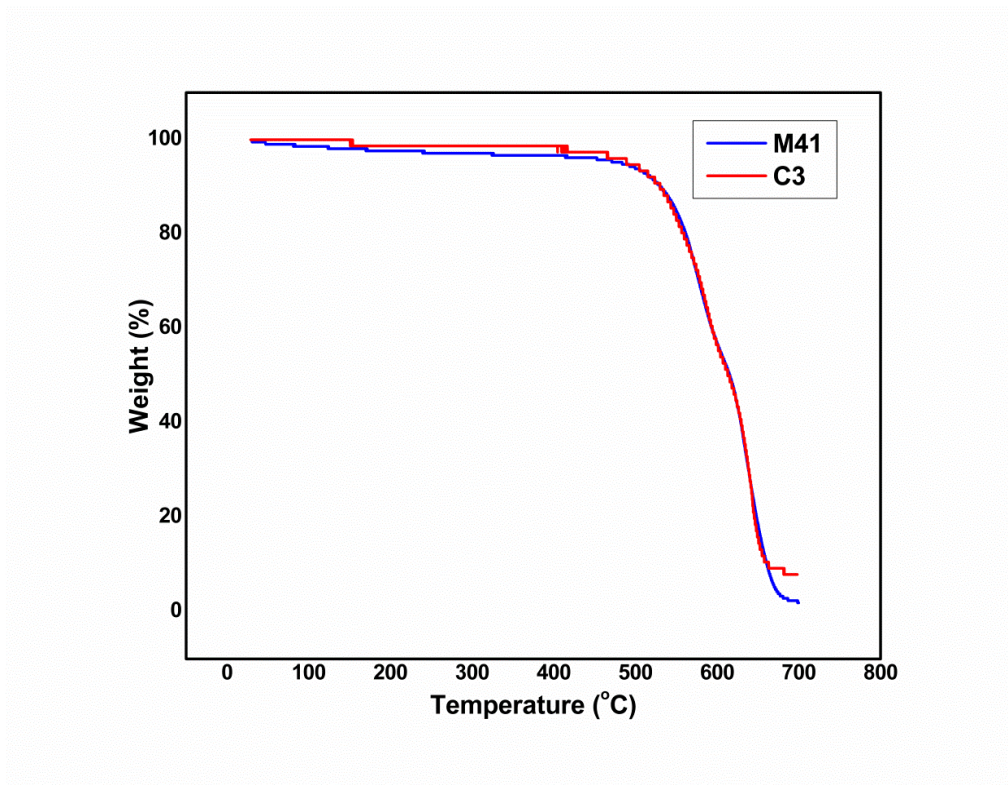


Figure 3.24 TGA spectra of unmodified azide functionalized MWCNT membrane [M41] and Click reaction modified membrane [C3]

3.10.3 Tensile strength

To understand the effect of chemical modifications on the bulk property like tensile strength, the tensile strength at break of the modified and unmodified unsupported membranes is given in Table 3.5. No significant change in the tensile strength of membranes after modification is observed. This again supports the earlier observation of the pore structure obtained, from FESEM, being unaltered after modification. The tensile strength is the maximum stress a material can withstand before break and young's modulus is the resistance of a material to elastic deformation under load which indicates that the modified membrane can

Chapter 3: Experimental route

withstand similar pressure in comparison to the unmodified membranes. The stress-strain curve is shown in Figure 3.25.

Table 3.5. Mechanical properties of azide functionalized MWCNT incorporated PES membrane [M41] and click reaction modified membrane [C3]

Code	Young's modulus (MPa)	Tensile strength (MPa)
M41	45.6	5.4
C3	137.4	5.8

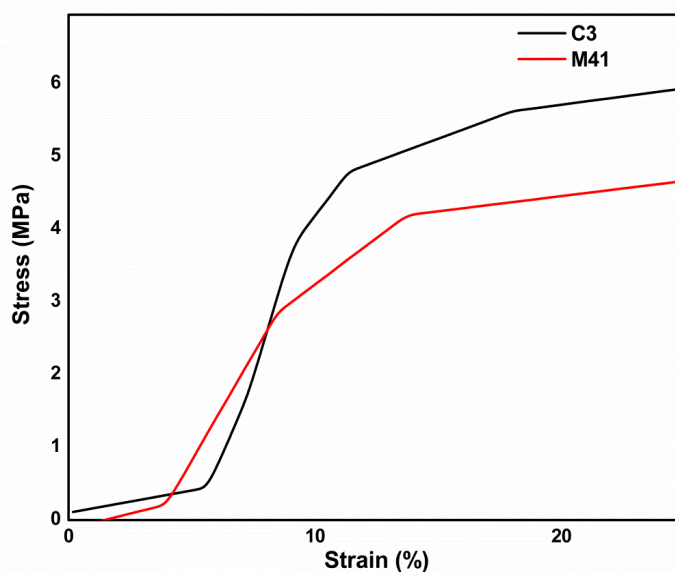


Figure 3.25 Stress-strain curves of azide functionalized MWCNT incorporated PES membrane [M41] and click reaction modified membrane [C3]